Direct search for WIMP dark matter

J. Gascon

DIRECT SEARCH FOR WIMP DARK MATTER

J. GASCON
Institut de Physique Nucléaire de Lyon, 4 rue Enrico Fermi
69622 Villeurbanne Cedex, France

We will review the experimental aspects of the direct search for WIMP dark matter. In this search, one looks in a terrestrial target for nuclear recoils produced by the impacts with WIMPs from the galactic halo. After describing the different ingredients involved in the calculation of rates in a given detector, we will present the different search strategies and review the currently running experiements and the prospects of future experiments.

1 Introduction

One of the most exciting possibility opened by the recent cosmological observations is that our Galaxy could be immersed in a halo of heavy Dark Matter particles of a fundamentally new type. In the most likely scenario these particles would be the WIMPs (acronym for Weakly Interacting Massive Particles). The discussion on how the WIMP has come to be one of the most actively sought hypothesis concerning Dark Matter has been discussed in other lectures in this school. A detailed discussion can be found in Ref. [1]. Here, we will review the experimental aspects of direct WIMP search. In this search, one looks, in a terrestrial target, for nuclear recoils produced by the impacts with WIMPs from the galactic halo. After describing the different ingredients involved in the calculation of rates in a given detector, we will present the different search strategies and review the currently running experiments and the prospects of future experiments.

As detailed discussions on this subject can be found in the literature, this short text is only meant as an introduction to the subject. For a more complete review on WIMP dark matter, we refer the reader to Ref. [1]. A comprehensive description of the method to interpret experimental WIMP search results can be found in Ref. [2].

2 Principles of Direct Detection

2.1 WIMP density

Cosmological measurements, such as those of WMAP[3], provide very strong incentives to look for dark matter. At these scales, the density of dark matter is of the order of 1 GeV/c^2/m^3, the equivalent in mass of one proton per cubic meter. In these measurements, dark matter signals its presence via gravitational effects on ordinary matter in the early universe. To clearly identify the nature of dark matter, it is crucial to be able to observe non-gravitational interactions with ordinary matter, or at least put an upper limit on the strength of these interactions. Only then would we able to test one of the most attractive scenario, namely that dark matter is made of Weakly Interacting Massive Particles, where "weakly" is meant in the context of the nuclear weak force. Two types of search are proposed: indirect or direct. Indirect searches look in cosmic rays for products of annihilation of WIMP pairs. This is discussed in more details in other lectures. Direct searches look for a nuclear recoil produced by a collision with a WIMP from the halo of our galaxy.

The rate of such collisions depend linearly on the local WIMP density ρ_{WIMP}. A common estimate[2] for this quantity is 0.3 GeV/c^2/cm^3. It should be noted that this local density should not be confused with the cosmological density of dark matter Ω_{DM}, which is also approximately 0.3 when expressed as a fraction of critical density of the universe. However the respective units differ by more than a factor of 10^6. One could have hoped that the improved accuracy of the recent measurements of Ω_{DM} would reduce the uncertainties in WIMP searches. This is not exactly the case, as ρ_{WIMP} is not derived from Ω_{DM} but from measurements of stars and gas in our galaxy, with cross-checks based on the rotation curves of other galaxies. However the cosmological measurements remain a strong incentive to look for local dark matter, as it would be surprising if this main component of matter in the universe remains absent of our neighborhood!

2.2 WIMP velocity

Assuming a local WIMP density of 0.3 GeV/cm^2, another ingredient is needed to estimate the WIMP flux in this room: their velocity distribution $f(v)$. The order of magnitude of their average velocity is fixed by the assumption that the halo WIMPs are gravitationnally bound to the galaxy (and its halo), leading to velocities of the order of stellar velocities in our galaxy, approximately 200 km/s. We will come back later on a more accurate description. For now, we can make the following order-of-magnitude calculation. For WIMPs with masses of approximately 100 GeV/c^2(the mass of a A=100 nucleus, we will see later the motivation for this example), the local density is 3000 WIMP per cubic meter, and a flux of 6×10^4 WIMPs is traversing each cm^2 of our body every second. Another important aspect is that the average kinetic energy of these WIMPs is 20 keV. This energy is much larger than the $\sim$eV scale binding energy of nuclei in a solid. In direct searches, the collisions are detected by the measurement of the energy of the recoiling nucleus, as its kinetic energy is dissipated in the detector medium. The simple kinematics of the collision is shown in Fig.1. In such a collision, the energy of the nuclear recoil E_{recoil} is given by:

$$E_{recoil} = E_{WIMP} \frac{4 M_{nucleus} M_{WIMP}}{(M_{nucleus} + M_{WIMP})^2} \cos^2 \theta_{recoil} \tag{1}$$

where $E_{WIMP}$is the initial kinetic energy of the WIMP, M_{WIMP} is its mass, $M_{nucleus}$ is the mass of the recoiling nucleus and θ_{recoil} is the angle of the nuclear recoil relative to the initial WIMP direction. From this equation, we can derive that the maximal recoil energy is obtained when

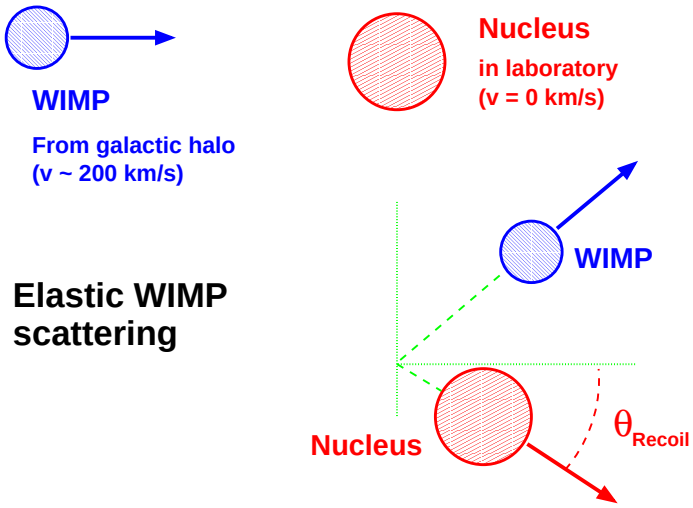

Figure 1: Kinematics of a WIMP-nucleus collision.

$M_{WIMP} = M_{nucleus}$. This search is thus more efficient for a WIMP with a mass comparable to nuclear masses.

As the resulting recoil energy depends on the kinetic energy distribution of the WIMPs in our halo, a more precise estimate of this velocity distribution is needed. Unfortunately, it is extremely difficult to calculate this distribution, even if we arbitrarily fix the total mass of the halo and neglect interactions with ordinary matter and non-gravitational interactions. The reason is that the gravitational force has an infinite range and the number of WIMPs to be included in the calculation is extremely large. The simplest case (see e.g. Ref. [2]) is to assume that the halo is spherical and that the WIMPs trapped in the galactic field have attained thermal equilibrium, with a Maxwellian velocity distribution:

$$\frac{dP(v)}{v^2 dv} = \frac{1}{(\pi v_0^2)^{3/2}} \exp(-\frac{v^2}{v_0^2}) \tag{2}$$

where v_0 ~220 km/s ($v_{rms} = \sqrt{\frac{3}{2}} v_0$ =270 km/s). To be consistent, this distribution is generally truncated at the velocity at which a WIMP could escape the galaxy (v_{escape} ~650 km/s). This model has many known shortcomings. It predicts a steep increase in density at the core of the galaxy that is not supported by observations. Many-body calculations also tend to produce non-uniform spatial density distributions (with so-called "clumps" of dark matter), with strong non-uniformity effects in phase space ("caustics"). In addition, the halo may not adopt a spherical shape (for example, it could be triaxial), and tidal flow from neighboring galaxies may play an important role. In view of these difficulties and in the absence of a consensus, the isothermal Maxwellian distribution is generally adopted for the analysis of dark matter searches. This is acceptable, as most searches are only sensitive to the average WIMP kinetic energy. This may evolve once a signal with significant statistics is observed.

With the simple Maxwellian distribution (eq.2), the relation between E_{recoil} and E_{WIMP} (eq.1) and the assumption of an isotropic θ_{recoil} distribution in the center-of-mass system of the collision, it is easy to derive the shape of the recoil energy distribution:

$$\frac{dN}{dE_{recoil}} \propto \exp(-E_{recoil}/ < E_{recoil} >)$$

where

$$< E_{recoil} >= \frac{\mu^2 v_{WIMP}^2}{M_{recoil}} \tag{3}$$

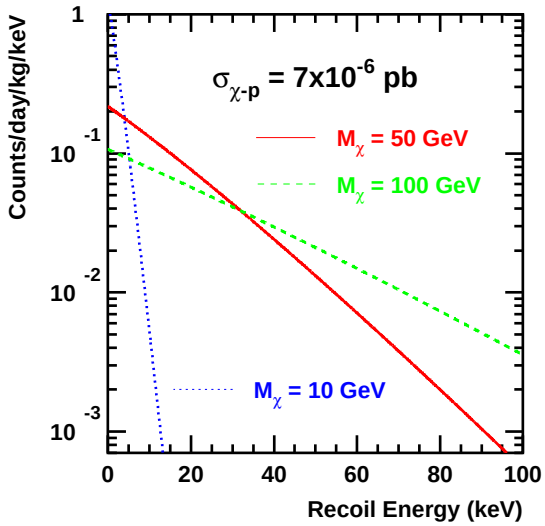

Figure 2: Recoil energy distributions for three different WIMP masses in germanium.

where v^2_{WIMP} is the average square velocity of the WIMP and μ is the reduced mass of the WIMP-nucleon system. Taking into account the finite escape velocity and the effects discussed in the following will not alter significantly this overall shape. Example distributions for different WIMP masses are shown for a germanium target in fig.2

A feature of the velocity distribution that is known with precision and can be easily implemented is the fact that the nuclear targets are not at rest relative to the galaxy, but are following the earth and the sun motions (fig.3). The tangential velocity of the sun around the galactic center (in the direction of Sagittarius) is 235 km/s. The net effect is to boost the average kinetic energy of the WIMP flux on earth. The earth velocity is an order of magnitude smaller (30 km/s) and can generally be neglected, except for an interesting modulation effect in the flux. As the earth orbits the sun with a 60^oangle relative to the galactic plane, a $30\times\cos 60^o$=15 km/s velocity component is alternatively added and subtracted to the sun's velocity relative to the WIMP flux. This may result in a $\pm 7\%$ annual modulation of the collision rate that can provide an interesting experimental signature of the astrophysical nature of the detected signal, although recent calculations have shown that the actual size of the effect may depend a lot on the details of the halo models (see e.g. refs.[4,5]).

To really make an efficient use of the modulation effects, a more powerful approach would be to detect for each recoil not only its kinetic energy E_{recoil} but also its direction θ_{recoil}. The apparent direction of the WIMP flux should be correlated with that of the motion of the sun around the galaxy, and have, in addition to the annual modulation, a diurnal modulation as the laboratory follows the earth rotation on its axis. However it is difficult to measureθ_{recoil}, as the typical recoil range of a recoil is of the order of 20 nm in a crystal (for a 20 keV Ge recoil in Ge, for example) and 30 μm in a gas (for a 20 keV Kr recoil in Kr). Detectors aiming at measuring the spatial extension of such short tracks are still at an early R&D stage (see e.g. DRIFT[6]). So far, the most sensitive experiments measure only E_{recoil} and are blind to the recoil direction.

2.3 Recoil Energy Measurement

Now comes the question of the method to detect the recoil energy. A nucleus with 20 keV kinetic energy will dissipate this energy in a crystal via three main processes: ionization, scintillation and phonons. The ionization corresponds to the electrons stripped by the initial nucleus and the following cascade. In certain material, this electronic activity will emit scintillation light. The

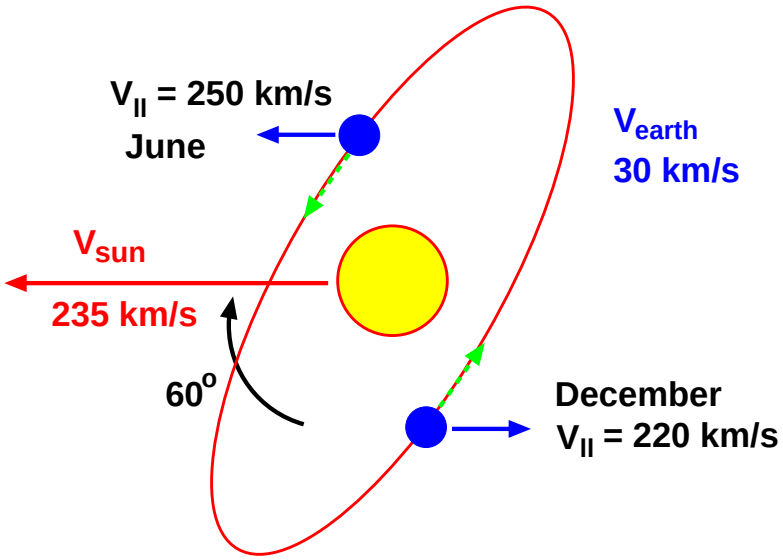

Figure 3: Earth and sun tangential velocity relative to the center of the Galaxy

movement of the incident nucleus in the lattice will also induce vibrational phonons. In a closed system, all ionization and scintillation energy will convert into phonons that will eventually thermalize and produce an elevation of temperature of the crystal.

In nuclear physics, the most common technique to detect radiation in the 20 keV range is the use of scintillating crystals (such as NaI or BGO) and solid state semiconductor ionization detectors (Ge or Si). However, these detectors are usually optimized for gamma-ray radiation and not nuclear recoils. When a keV to MeV range photon enters an detector, it converts most of its energy to an electron. The range of this electron is of the order of the μm , much greater than the nm range of nuclear recoils, and as a consequence, this electron will produce more ionization than a nuclear recoil of equal energy, as the latter will lose a substantial part of its energy directly into phonons associated with atom vibrations as the nucleus is stopped in the lattice. Scintillation yields of electron and nuclear recoils will be similarly affected. A quantitative measure of this effect is the so-called *quenching factor* (symbol: Q). Its definition is the following. First, the ionization, scintillation or heat response of a detector to gamma-ray of known energy is measured, yielding a calibration of the signal in keV-equivalent-electron (keV$_{ee}$). Then, the response of the detector to a nuclear recoil of known energy E_{recoil} is measured. As the ionization or scintillation yield will be lower than in the electron recoil case, the measured signal in keV$_{ee}$ will be $E_{ee} = QE_{recoil}$, where Q is a fraction. With this definition, Q is the relative signal yield for nuclear and electron recoils. For a recent review of quenching measurements, see Ref.[7] and references therein. For the heat measurement in perfectly isolated detectors, Q should be unity, if one waits long enough for the complete thermalization of all energy. In ionization detectors such as Ge or Si, $Q \sim 0.3$, with a moderate energy dependence. For scintillation, there is a wider range of values: in NaI, the quenching for Na and I recoils are ~ 0.25 and~ 0.09, respectively. Another noteworthy case is scintillation in Xe ($Q \sim 0.2$). The quenching factor must be kept in mind when comparing different detector results, as the measured energies are often quoted in keV$_{ee}$ instead of true recoil energy. More interestingly, as will be shown later, this effect can be put to contribution as a mean to discriminate nuclear recoils from the usually large background of electronic recoils.

2.4 Order-of-magnitudes of scattering cross-sections

In order to estimate the rate of collisions between WIMP and nucleons, one needs to define which elementary force mediates these encounters. Gravitational interactions between a single WIMP and a single nucleus are negligible. Electromagnetic interactions are excluded, since it would mean that WIMP could emit or absorb light. However, it has been observed that the behavior of the dark matter particles throughout the Big Bang up to now could be explained by simply assuming that they only participate to weak interactions. If this is the case, this leads to an estimate of the probability of a collision with a nucleus.

In particle and nuclear physics, the probability of an interaction is usually expressed as deriving from a *cross-section*, σ, with units of surface. If dN/dt is the number of WIMP-nucleus interactions per unit time, ϕ is the WIMP flux and the number of target nuclei per volume, we have

$$\frac{dN}{dt} = \phi \sigma_A N_{target}$$

where σ_A is the cross-section for a WIMP-nucleus collision. A typical cross-section for a collision on a $A \sim 100$ nucleus involving the nuclear force only is of the order of the size of this nucleus: $10^{-24}\text{cm}^2 = 1$ barn (symbol: b). Collisions involving electromagnetic interactions will have a much larger cross-section, due to the long-range nature of the force. If the nuclear Weak force is involved, the cross-section is at most 1 picobarn (1 pb = 10^{-12}b). Typical weak cross-sections on single nucleon (a proton or a neutron) are even lower than this ($\sigma_n \sim 10^{-7}$pb). With such cross-sections, the interaction rate with the WIMP flux can be expected to be at most one collision per kilogram of matter per day, possibly as low as one per year and per ton of detector.

2.5 Scaling from a nucleon to a nucleus

The reason why the weak cross-section on a $A = 100$ nucleus is not simply 100 times that on a single nucleon is that the wavelet associated to the momentum transfer corresponding to a A=100 nucleus with 20 keV kinetic energy is approximately 3 fm, about the size of the entire nucleus. In this case, one must evaluate whether the interaction goes through a spin-dependent or scalar (spin independent) process. In the first case, only the unpaired nucleon will contribute significantly to the interaction, as the spins of the A nucleon in a nucleus are systematically anti-aligned. In the second case, all nucleon contributions add coherently: the total amplitude scales as A and the total scattering probability as A^2. Another mass-dependence hidden in the scaling from σ_n to σ_A is that interaction probability depends on the density of states in the final state, which in this case[8], implies that $\sigma_A/\sigma_n = \mu_A^2/\mu_n^2$, where μ_A (μ_n) is the invariant mass of the WIMP-nucleus (WIMP-nucleon) system. In summary, the $A-$dependence of WIMP-nucleus cross-section is:

$$\sigma_A = \frac{\mu_A^2}{\mu_n^2}\,\sigma_n\,A^2 \,\text{(spin independent)}$$

$$\sigma_A = \frac{\mu_A^2}{\mu_n^2}\,\sigma_n C\,J(J+1)\,\text{(spin dependent)}$$

where C is a factor that depends on the details of the structure of the nucleus[2]. It cannot be expressed in a simple form, but is generally less than unity.

As $\mu_A^2/\mu_n^2 \sim A^2$, the interaction rate per kilogram of target mass is proportional to A^3in the case of spin-independent interactions and only to A in the case of spin-dependent interactions. Direct searches try to benefit from this scaling by using targets with as large A as possible. In any model where some part of the interaction involves spin-independent interactions, this term dominates the cross-section.

2.6 Nuclear form factors

It was stated that the advantageous A^2 scaling of the spin-independent cross-section arises from the fact that the wavelength associated with the momentum transfer is comparable to the size of the nucleus. To be more precise, full coherence is only achieved when the associated wavelength is much larger than the nucleus size. In the present case, one has to take into account interference effects that can be calculated rather precisely using the known form factors. The nuclear structure models behind these calculations and the size of the effect are discussed in Ref.[2]; here it suffices to say that the net effect in most commonly used target material is to reduce the interaction rate by a factor of 2 to 4, which damps the increase due to the A^2dependence when $A \sim 100$.

2.7 Supersymmetric models predictions

With precise prescriptions on the choice of ρ_{WIMP}, $f(v)$, the σ_A/σ_nscaling and the nuclear form factor, the only two missing ingredients for predicting the WIMP rate in a given detector are M_W and σ_n. For these, one needs a model with specific predictions on the nature of the WIMP.

More precise predictions on the interaction rates can be obtained within the framework of Supersymmetry (SUSY). In fact, this theory actually predicts very naturally that there exists a heavy neutral particle (called the neutralino, with symbol χ^0) with weak interaction only, that was created copiously at the Big Bang. And this, quite remarkably, even though the theory was not motivated as to fix the dark matter problem, but to solve basic problems in the quantum description of the behavior of elementary particles. The great advantage of this model is that its predictions are somewhat constrained by the results of searches for supersymmetric particles and for deviations from the Standard Model of interactions. For example[1], the mass of the neutralino cannot be much greater than 1 TeV/c^2. It cannot be less than 50 GeV/c^2, except in exceptional versions of the model that are specially tuned for this purpose[10]. In addition, models with purely spin-dependent interactions are essentially ruled out, and in this framework, large-A detectors are clearly favored. Fig.4 shows the range of M_W and σ_n allowed by different versions of SUSY models. In addition to these so-called "scans" of different versions[10,11,12] of the Minimum Supersymmetric Model (MSSM), other calculations[13] offer "bench mark models" that explore interesting cases. Typical values of σ_n are in a 10^{-11} to 10^{-7} pb. This is a few order of magnitudes below the sensitivity achieved by current detectors[18,22,23], also shown in Fig.4.

3 Search Strategies

3.1 Search sensitivities

However, as it can be seen in Fig.5, a sensitivity of the order of 10^{-10}pb is within the reach of a one-ton size detector running over a full year with a perfect rejection of background, and with a recoil energy threshold of 20 keV. Detectors with large-A targets are favored over light-A target such as Ne ($A = 20$). As described in the previous section, increasing A from ^{73}Ge to ^{131}Xe does not improves the sensitivity because of the evolution of the nuclear form factor and also because of the $1/M_{recoil}$ dependence of the average recoil energy (Eq.3). As expected from kinematics, the experiments are the most sensitive for $M_W \sim M_{nucleus}$. At lower masses, the presence of a fixed recoil energy threshold further deteriorates the performance of the search.

For a $M_W = 100$ GeV/c^2, a cross-section of 10^{-6} pb correspond to approximately 0.1 collisions per kg per day (kg·d); cross-sections of 10^{-8} and 10^{-10} pb corresponds respectively to 0.5 events per kg per year (kg·y), and 5 per ton and per year (t·y).

The sensitivities of these ideal experiments are calculated the following way. If no events are observed in the ton of target over the year, an upper limit with a 90% confidence level can be

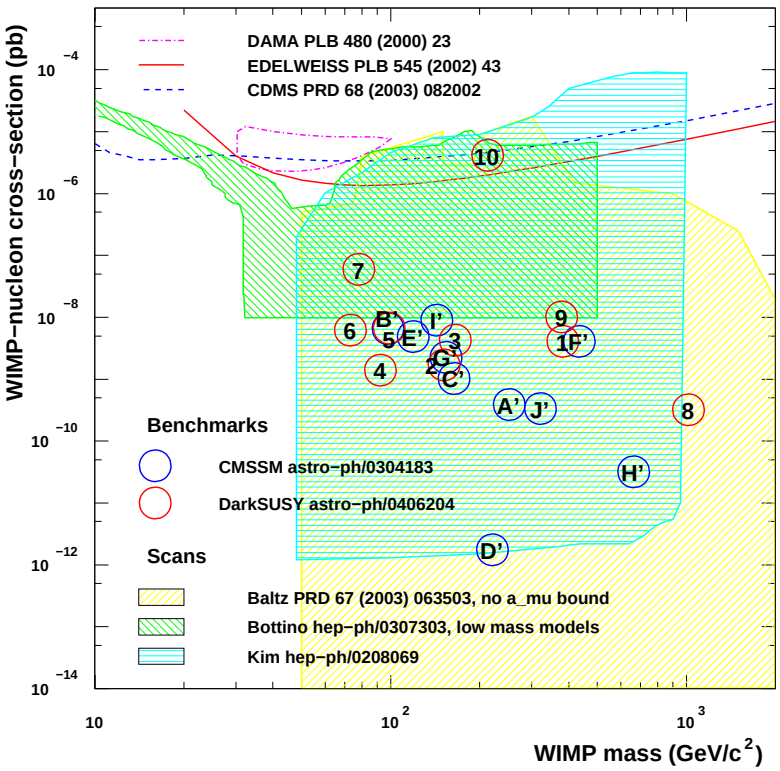

Figure 4: Predicted ranges of M_W and σ_n in different supersymmetric models. Published sensitivities of some experiments are shown as a comparison. See text for references.

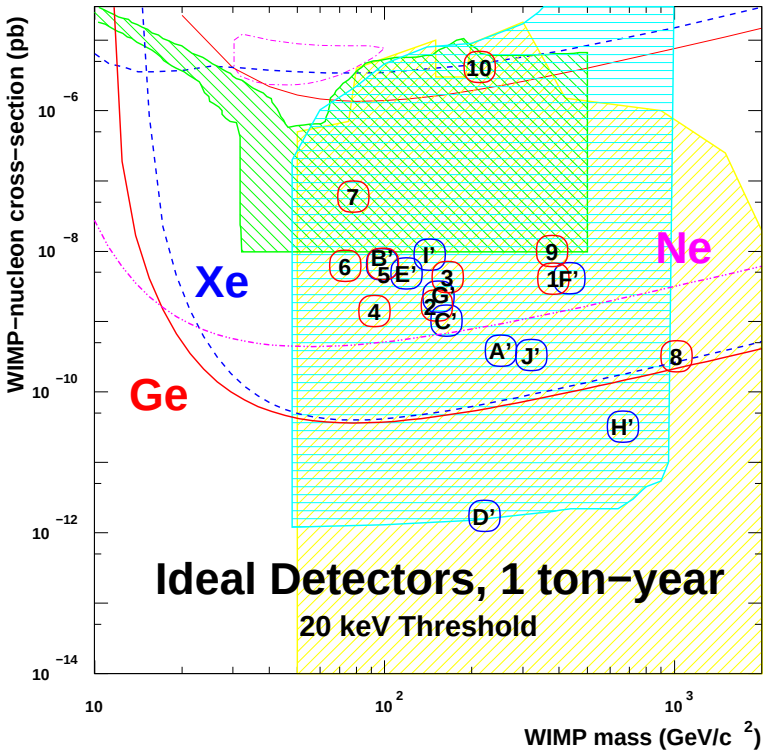

Figure 5: Sensitivity of a one-ton size detector running over a full year with perfect background rejection. The supersymmetric predictions are those of Fig.4.

ascribed to σ_n. Lets call this limit $\sigma_n^{90\%}$. This 90% confidence level (C.L.) means that in the case that $\sigma_n = \sigma_n^{90\%}$, the probability of having a one ton-year experiment with zero observed events is 10%. In the 90% other cases, the number of observed events would be 1, 2 or more. The probability distribution of this background-less experiment is given by the Poisson distribution[9]:

$$P(n,\mu) = \frac{\mu^n}{n!}\exp(-\mu)$$

where $P(n,\mu)$ is the probability of observing n events in a random process where the average number of observed events is μ. $P(0,\mu) = 0.9$ correspond to $\mu = -\ln(1-0.9) = 2.30$, so that $\sigma_n^{90\%}$corresponds to the cross-section that would yield on average 2.30 events in the detector. The lines drawn on Fig.5 correspond to $\sigma_n^{90\%}(M_W)$.

In the presence of a background, the sensitivity deteriorates significantly. In the limit that the number of observed background counts n_{bkg} is large, the sensitivity as measured by $\sigma_n^{90\%}$ becomes equal to the cross-section yielding on average n_{bkg} events in the detector. As the time increases, so does n_{bkg} and an increased exposure does not yield a better sensitivity. Even if the background can be evaluated precisely by an independent measurement and subtracted from the number of observed events n, the statistical Poisson fluctuations on n remains. In this case the sensitivity $\sigma_n^{90\%}$ corresponds to the cross-section predicting an average number of observed signal events of $1.28\sqrt{n_{bkg}}$, if $n_{bkg} <\sim 20$. As the exposure increases, the sensitivity grows very slowly with time ($\sqrt{t}$).

3.2 Low backgrounds

Extremely low background levels are thus essential for reaching sensitivities covering the range of the MSSM predictions. As a comparison, the radioactivity of a human body represents 10^7 decays per kg·d, with most of them depositing more than 100 keV of energy. This is very far from the 0.1 decays per kg·d necessary to achieve a 10^{-6} pb sensitivity. The background from natural radioactivity has two sources: external and internal radioactivity.

The shielding from external sources of radioactivity is achieved by surrounding the detector with thick walls of absorbing material. A high-Z material like lead is very effective for stopping MeV-energy gamma-rays, while a few mm of low-Z material are sufficient for stopping low-energy gamma-rays as well as beta and alpha radiations. Beyond a thickness of 15 to 25 cm of lead, one is generally limited by the internal radioactivity of lead itself. Fast neutrons are not by number a large part of natural radioactivity, but they are of concern in direct searches, as they produce nuclear recoils similar to those produced in WIMP collisions. Fast neutron shields consist moderators made of material with a high density of hydrogen, such as polyethylene or water.

Good internal radioactivity is achieved by using detectors made of radiopure material. This limits the choice of detector technology. In addition, it is necessary to place the detector in a deep-underground site, where it is protected from the penetrating cosmic muon flux. At ground level, this radiation (approximately 10^3 muons per cm^2 per day) induces nuclear transmutations to unstable isotopes throughout the detector volume. In underground laboratories such as Soudan Mine in Minnesota, the Gran Sasso laboratory in Italy or the Laboratoire Souterrain de Modane in the Fréjus Tunnel, this flux is reduced by a factor varying from $10^5$to 10^7(see Fig.6).

3.3 WIMP signatures

To these passive shielding setup, one generally adds active background rejection techniques, where an energy deposit due to a non-WIMP source is identified by their different signatures. The two extreme cases of background rejection are the *event-by-event rejection*, where each energy deposit in the detector is associated to an additional signal that can be used to reject

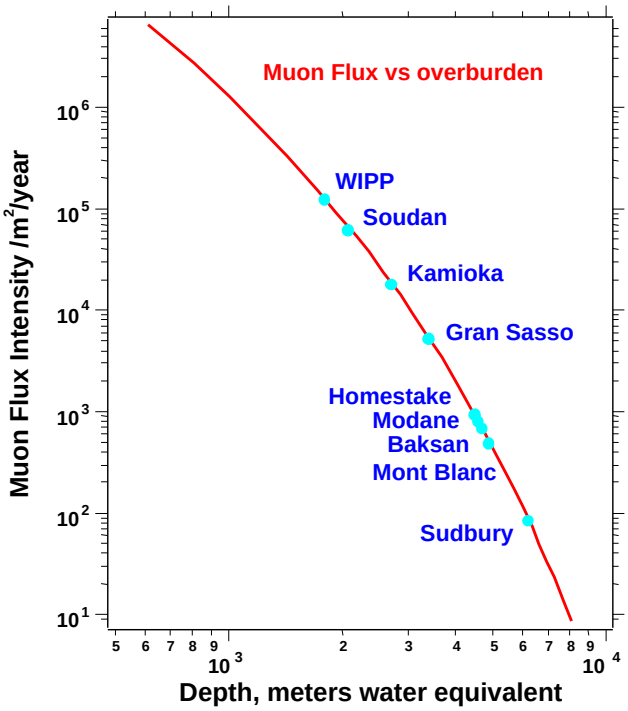

Figure 6: Muon flux in muons per m^2per year and per steradian in different underground laboratories.

background events with a 100% certainty, and the *statistical rejection*, where the additional information can be used to ascertain which fraction of the total event sample comes from a well-defined type of background, but cannot tell for one individual event. In the second case, the precision on the WIMP rate is limited by the statistical fluctuation on the total sample, background included. The first case is ideal, as in practice there is always a small probability that a background may fake the signature of a WIMP. However, if this probability is small and the expected number of fake WIMPs is less than one, the rejection can be considered to be truly made event-by-event. Available WIMP signatures are:

Nuclear recoils: WIMPs produce nuclear recoils, while most radioactive backgrounds interact via the electromagnetic force and produce electron recoils. The discrimination of nuclear and electron recoils is generally based on the fact that the former have a larger energy loss per unit length (dE/dx) and a smaller recoil range. This also leads to the previously discussed quenching effects, as well as difference in scintillation time constants in some crystals.

The shape of the recoil energy spectrum: The shape of the E_{recoil} spectrum for a WIMP with a given mass can be calculated rather precisely. The observed energy spectrum must be consistent with the expectation. Even if few events are expected, the predicted spectrum shape is a useful tool to define the optimal E_{recoil} search range, which may vary as a function of M_W. However, the overall shape is exponential, as is the case for many background sources.

Coherence: For spin-independent interaction, the scattering cross-section should be proportional to $\mu^2 A^2$. The observed rates in different detectors should obey this law. For example, the scattering cross-section of fast neutrons is approximately equal to the geometrical cross-section of the target nucleus, and corresponds to a $A^{2/3}$ dependence.

Multiple interactions: The mean free path of a WIMP in matter is of the order of a light-year, so the probability of two consecutive interactions in a single detector or two adjacent detectors is completely negligible. In comparison the mean free path of a high energy gamma-ray or a neutron is of the order of the cm and multiple interactions are more common. An array of closely packed detectors can efficiently identify these backgrounds.

Uniform rate throughout the detector: The long mean free path of WIMPs also means that their interactions must be spread evenly throughout the detector volume. If the detector size is significantly larger than the mean free path of high-energy photons or neutrons, the interaction of the radiation originating from the surrounding material and surface contaminant will occur mostly at the detector surface. This leads to the incentive of building large position-sensitive detectors. Other type of radiation have very short mean free path (<mm), such as low-energy photons, beta and alpha rays, and can be rejected even if the position sensitivity is limited to the identification of energy deposits located near the surface of the detector.

Annual modulation: As discussed in section2.2, the WIMP flux and its average kinetic energy modulates annually as the earth alternatively adds and subtracts its velocity to the sun movement relative to the galaxy. In the absence of annually-modulated backgrounds, this behavior may be used as a WIMP signature, although the size of the modulation is more dependent on the details of the halo model than the year-averaged rate. Another drawback is that the statistical uncertainty on the modulated signal is dominated by the contribution of the large non-modulated component of the WIMP rate. For example, even in the total absence of background, a 3σ measurement (33% relative error) of a $\pm 2.5\%$ modulation of the rate requires a sample of at least 36000 WIMPs. Current background-free experiments are excluding at 90% C.L. rates corresponding to 0.2 events per kg·d, with exposures of the order of 10 kg·d. Consequently, the observation of a 3σ modulation effect would require an exposure greater than half a ton-year!

Directionality: see section 2.2.

In order to be convincing, an eventual WIMP signal should combine more than one of these signatures. In addition, the results of direct searches should be compatible with those of indirect searches, and with the properties of the type of neutralino that would be eventually discovered at the Large Hadron Collider.

3.4 Current status of direct searches

Fig.7 shows the evolution as a function of time of the sensitivity for a 60 GeV/c^2 WIMP of different direct searches. The different detector techniques will be described in turn in the next section. Published results are shown as full symbols and lines. Preliminary results are shown as open symbols and dashed lines, while projections and estimates are represented with crosses and dotted lines. At present, the most competitive direct searches have reached sensitivities close to 10^{-6} pb. This starts to explore the domain of optimistic Supersymmetric models. In the coming years, different projects are planning to reach sensitivities approaching 10^{-8} pb. This represents a factor 100 increase in performance. This phase should help identify which technologies are suited for the next ambitious goal, to achieve a further factor 100 in performance and reach 10^{-10} pb-scale sensitivity with ton-scale detector arrays. Only then will we be able to cover most of the predictions of supersymmetry.

4 Review of Present Experiments

4.1 Ionization

Already used in the first early WIMP searches, Ge ionization detectors benefit from the high intrinsic purities achieved by the semiconductor industries and from the developments in the context of the search of the neutrino-less double-β ($0\nu 2\beta$) decay of ^{76}Ge. Despite the impressively low raw rates obtained by the Heidelberg-Moscow[14] and IGEX[15] experiments, the lack of event-by-event rejection of electronic recoils means that the sensitivity of this technique, now limited to approximately $\sim$1 event per kg·d for WIMP searches, can only be improved by further efforts on the radiopurity of the detector environment and by the exploitation of the self-shielding

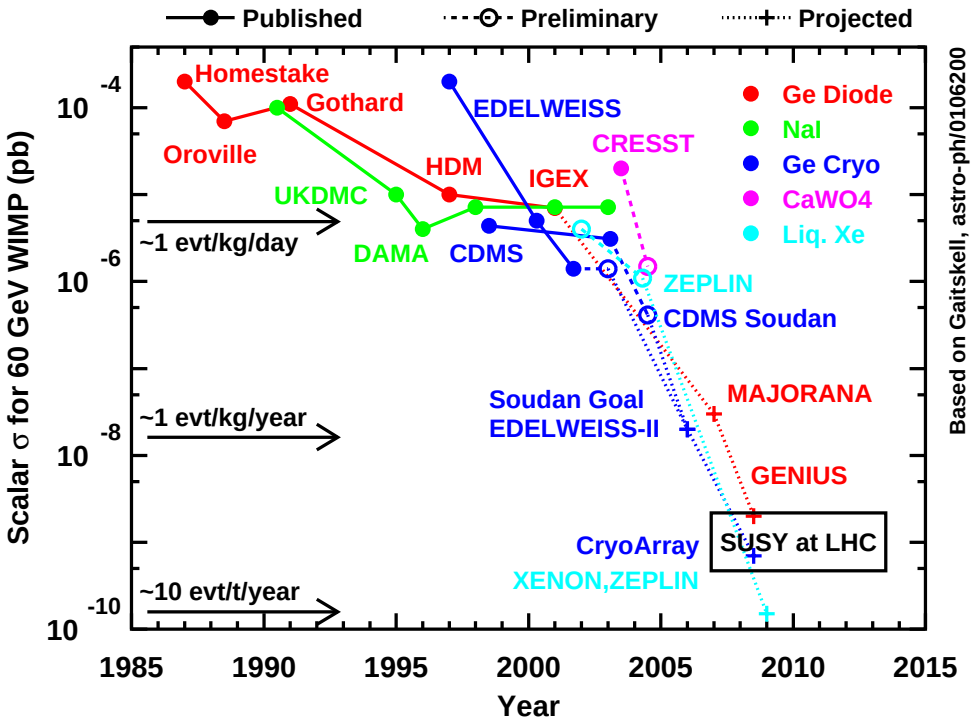

Figure 7: Status and evolution of current direct searches experiments. See text for explanation.

possibilities offered by large and compact arrays of detectors. With a strong motivation in the context of $0\nu2\beta$ decay searches, two ton-scale arrays are being developed: GENIUS[16], with naked Ge detectors immersed in liquid nitrogen, and MAJORANA[17]. This project is developping detectors with highly segmented electrodes, with the intent of identifying multi-hit events by the study of the shape of the pulses on the different segments. This technique is well suited for the rejection of the multiple Compton scattering events produced by the$\sim$2 MeV photons which constitute an important source of background in the $0\nu2\beta$ decay searches. More studies are needed to evaluate its suitability to the low-energy signals associated with WIMP-induced nuclear recoils.

4.2 Scintillating Crystals

Scintillating crystals like sodium iodine (NaI) are a convenient solution to accumulate large masses on detector material. It is however more difficult to achieve radiopurity comparable to Ge. NaI-based searches, such as DAMA[18], ELEGANT[20] or NAIAD[19], originally attempted to use pulse shape discrimination to statistically identify a WIMP component in their observed rate. It was found that the low number of detected scintillation photon per keV of incident energy ("photo-electron per keV", or p.e./keV$_{ee}$) restricts the usefulness of this method at low energy. The technique is now being investigated for CsI scintillator[21], where the difference in time constants between electron- and nuclear-recoil induced scintillation is larger than in NaI.

The limitation of pulse shape analysis at low energy enticed the DAMA collaboration to turn to a statistical discrimination based on annual modulation[18]. With a data set of 10^5 kg·d recorded with a 100 kg array of NaI over eight years, DAMA reports the observation of a modulation originally interpreted as a WIMP with $M_W = 52$ GeV/c^2 and $\sigma_n = 7.2\times10^6$pb. Such a WIMP corresponds to a total rate of approximately 1 nuclear recoil per kg·d above a threshold of 2 keV$_{ee}$ corresponding to approximately 22 keV recoil energy. Reconciliating the reported modulation effect with the published exclusion limits based on cryogenics Ge detectors[22,23],

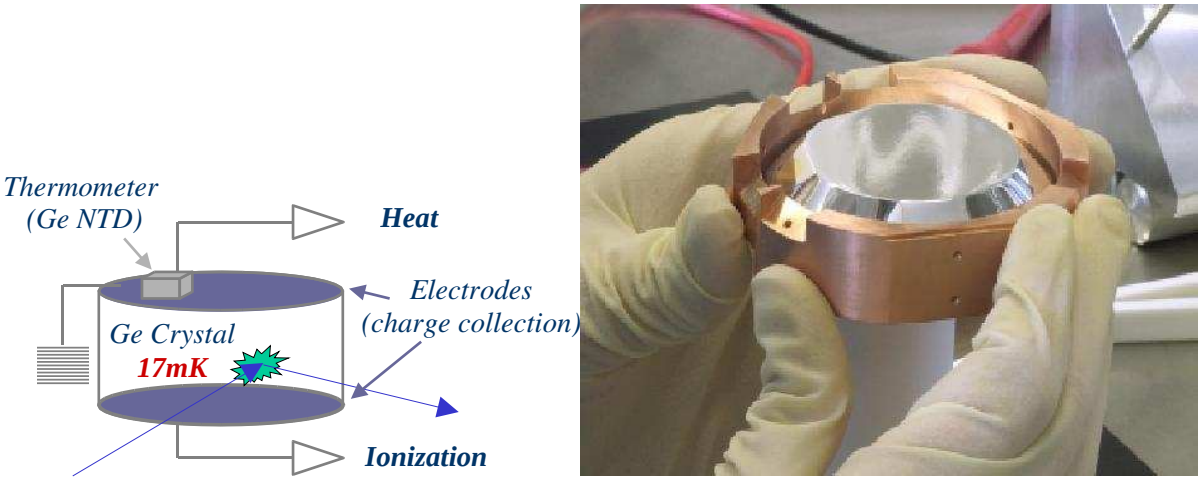

Figure 8: Left: schematics of the heat-and-ionization detector of the EDELWEISS collaboration (see text). Right: picture of a detector in its copper support frame, before the wiring of the electrode and the NTD heat sensor.

and with indirect search results requires very strong excursions from the usual supersymmetric neutralino scenario[4,24]. DAMA is nevertheless planning an upgrade to a larger mass of detectors (LIBRA).

4.3 Noble Liquids

Noble liquid scintillating detectors can provide large volume of highly purified target material. Xenon[25,26,27] is particularly interesting because of its high-A value, but argon[28] and neon[29] are also studied. Despite the development of very efficient purification techniques developed for noble gases (originally, to improve the stability of the scintillation properties), surface radioactivity from the liquid container and the signal extraction system is to be expected and some event-by-event background rejection is required.

For xenon, different strategies are being investigated. The ZEPLIN collaboration[25] has reported results from pulse shape discrimination based on the different scintillating time constants of nuclear and electron recoils in a 6 kg liquid Xe cell. However, it is now moving to a two-phase (liquid+gas) detector, where the main discrimination comes from the difference in ionization and scintillation yields of electron and nuclear recoil events. A strong electric field drifts the ionized electrons out of the liquid phase into the gas phase, where they are detected via the secondary luminescence. The collaboration XENON[26] is preparing a 100 kg two-phase project, with nuclear/electron recoil discrimination coming from the ionization/scintillation yields, and will exploit the position-dependence of the signals to define a fiducial volume away from surface contaminations. Another Xe project is XMASS[27], where the emphasis is put on position resolution in order to reject events due to surface contamination and multiple scattering inside the 100-kg detector.

4.4 Bolometers with Discrimination

With this type of detector, the emphasis is on event-by-event rejection of electronic recoils using the difference in quenching effects between the phonon/heat signal and either the ionization or the scintillation signal. As an example, Fig.8 shows the schematic view of the heat-and-ionization of the EDELWEISS collaboration[22]. An energy deposit in the detector will result in the creation of electron-holes pairs in the semiconductor crystal, collected on Al-sputtered electrodes polarized at a bias of a few Volts. In a few ms after the interaction, the entire incident energy is thermalized in the detector, cooled down to 17 mK in order to reduce the

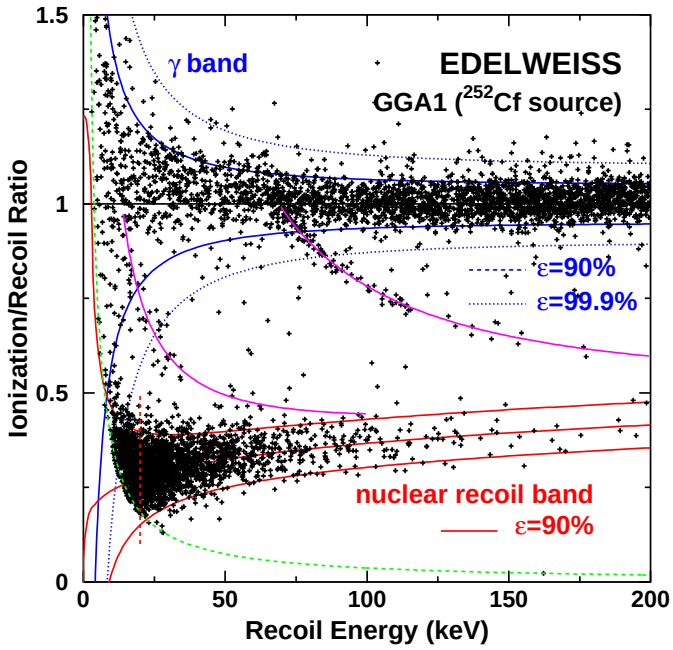

Figure 9: Distribution of the the quenching factor (ratio of the ionization signal to recoil energy) as a function of the recoil energy recorded with a 320 g EDELWEISS detector exposed to a ^{252}Cf source emitting neutrons and photons. The full lines correspond to the $\pm 1.645\sigma$ bands (90% efficiency) for electronic and nuclear recoils and the dotted lines to the $\pm 3.29\sigma$ band (99.9% efficiency) for electron recoils.

heat capacitance of the crystal an produce a temperature increase of a few μK, measured with a Neutron Transmutation Doped Ge thermistance glued to the side of the detector. With the simultaneous measurement of the heat and ionization signals for each event, one can deduce the true recoil energy and the ionization quenching associated to it. Fig.9 shows that this technique can discriminate efficiently nuclear and electron recoils, down to low recoil energy.

The ZIP detectors developed by the CDMS collaboration are based on the same principle, except that the heat sensor is replaced with a thin film sensor able to detect phonons before their complete thermalization. As discussed later on, the detection of this fast component leads to the possibility to identify energy deposit close to the surface by using the time evolution of the rise of the phonon signal.

The heat-and-ionization technique have come to a mature stage and are now providing the best published sensitivities of $\sim$0.2 nuclear recoil per kg·d, achieved by the EDELWEISS[22] and CDMS[23] cryogenic Ge detectors (3$\times$320 g and 4$\times$160 g, respectively). More than 99.9% of the electronic recoils are rejected down to 15 and 10 keV, respectively. Since then the two experiments have presented updated preliminary results.

EDELWEISS has increased its total exposure from 11.7 kg·d to 62 kg·d, and has reduced its threshold to 11 keV recoils. In total, 3 events are observed in the critical 30 to 100 keV range. More events (34) are observed at lower energy. The 90% C.L. limits on σ_n deduced from the observed events is essentially the same as those from the smaller published data set, as can be seen on Fig.10. A coincidence between two detectors, with both hits being identified as nuclear recoils, indicates that a residual neutron background is likely present, and the WIMP limits, derived with no background subtraction, are conservative. The installation of the next phase of the experiment is now under way. It will involve 28 detectors, with 7 being equipped with NbSi

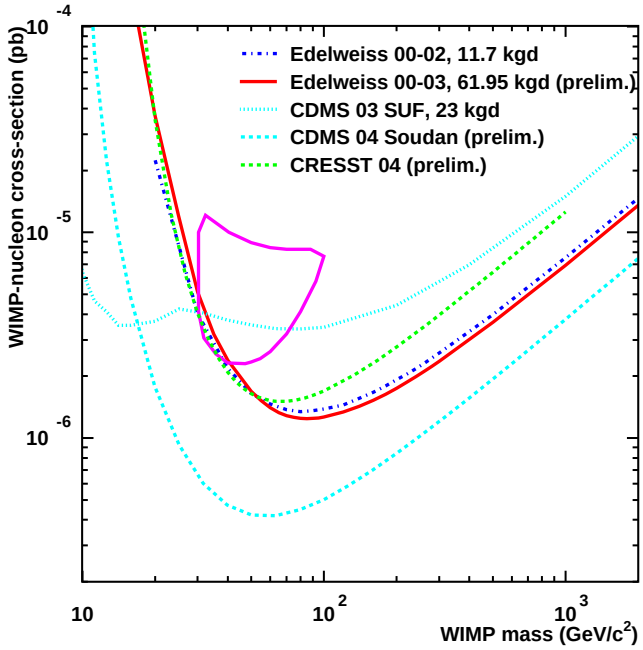

Figure 10: 90% C.L. confidence limits on the spin-independent WIMP-nucleon cross-section as a function of the WIMP mass for the different cryogenics experiments described in the text.

thin film sensors, the latter being able to use athermal phonon detection for the rejection of the near-surface events that may yield deficient ionization signals.

Recently, CDMS[30] has presented preliminary results obtained with four 150 g Ge detectors equipped with athermal phonon sensors, operated at the SOUDAN underground site. After cuts on the timing information to remove surface events, an exposure of 19.4 kg·d is obtained with at most one event observed in the 10-100 keV range. The resulting 90% C.L. limits, shown in Fig.10, are the first to go below the 10^{-6}pb sensitivity.

Another exciting development is the preliminary results[31] obtained by the CRESST collaboration with heat-and-scintillation detectors[32]. In their 300 g $CaWO_4$ detector, the ratio of the scintillation signal to the heat signal provides a 99.9% rejection of electron recoils. In addition, their preliminary measurements of the relative light yields of Ca, W and O recoils indicate that the light yield for W recoils is significantly less than for Ca or O recoils. In this detector one expects not two but three distinct populations: electron recoils, O and Ca recoils (primarily due to neutron scattering) and W recoils. Because of the $\mu^2 A^2$ dependence, WIMPs are expected to interact primarily with W nuclei, while neutrons will interact relatively more often with O and Ca nuclei. The observation of no events in the W recoils band in the interval from 12 to 40 keV in a 10.5 kg·d exposure yields the preliminary 90% C.L. limit shown on Fig.10.

CDMS-II and CRESST-II are both pursuing their data taking with 10^{-8}pb sensitivity goals, as for EDELWEISS-II, which will resume its operations in 2005. For the 10^{-10}pb horizon, one-ton size cryogenics arrays of detectors are being studied by both CDMS (CRYOARRAY[33]) and CRESST-EDELWEISS (EURECA).

4.5 Other techniques

This review of the experimental techniques was focused on those that have lead, in the past, or are currently leading the field of direct dark matter searches in the context of the minimal supersymmetric models. It is in no way exhaustive. As current experiments are more than four order of magnitude away from a full coverage of the bulk of supersymmetric predictions, the

coming years may reveal that the ultimate sensitivity can only be reached by detector techniques that are now in a very early development stage. For example, detectors sensitive to the recoil direction such as low-pressure Time Projection Chamber (see e.g. Ref.[6]) may be essential for the exploration of the kinematics of the WIMP flux on earth. Or it could be that the WIMPs do not follow strictly the behavior suggested by the most common forms of the supersymmetric models. For example, if the WIMP would interact almost solely via spin-dependent interactions, detectors made of nucleus with a large intrinsic spin, like those developed by the PICASSO and SIMPLE collaborations[34], could play a more important role.

5 Conclusions

The field of direct WIMP search is stimulating an intense detector development effort aimed at achieving the sensitivity required for the extremely low rates and low energy involved. Cryogenic detectors with event-by-event identification of nuclear recoils have for now taken the lead in this domain, but there is still a lot of development in progress on the road to the 10^{-8}pb sensitivity of current projects to the ultimate 10^{-10}pb sensitivity necessary to cover most of the MSSM domain. In fine, only a combination of experimental signatures, and thus likely of different detector techniques, will produce a satisfying positive identification of the true nature of the WIMP.

Acknowledgments

Je remercie les organisateurs de l'cole pour leur invitation et les flicite pour leur succs.

1. G. Jungman, M. Kamionkowski and K. Griest, Phys. Rep. **267**, 195 (1996).
2. J.D. Lewin and P.F. Smith, Astropart. Phys. **6**, 87 (1996).
3. D.N. Spergel *et al*, Astrophys. J. Suppl. **148**, 175 (2003).
4. C.J. Copi and L.M. Krauss, Phys. Rev. D **67**, 103507 (2003).
5. A.M. Green, astro-ph/034446.
6. D.P. Snowden-Ifft, T. Ohnuki, E.S. Rykoff and C.J. Martoff, Nucl. Instr. Meth. A **498**, 155 (2003).
7. E. Simon *et al,* Nucl. Instr. Meth. A **507**, 643 (2003).
8. See e.g. Eq. 4.8 in Introduction to High Energy Physics by D.H. Perkins, 1987, Addison-Wesley Publishing, USA.
9. See e.g. sections 28 and 29 of the Review of Particle Physics by the Particle Data Group, Eur. Phys. J. C 3 (1998) 1.
10. A. Bottino, F. Donato, N. Formengo and S. Scopel, Phys. Rev. D 69 (2004) 037302.
11. E.A. Baltz and P. Gondolo, Phys. Rev. D 67 (2003) 063503.
12. Y.G. Kim, T. Nihei, L. Roszkowski and R.R. deAustri, JHEP 0212 (2002) 034.
13. J. Ellis, astro-ph/0304183;
    P. Gondolo, J. Edsjö, P. Ullio, L. Bergström, M. Schelke and E.A. Baltz, astro-ph/0406204.
14. H.V. Klapdor-Kleingrothaus *et al*, HDMS Collaboration, Astropart. Phys. 18 (2003) 525.
15. A. Morales *et al*, Phys. Lett. B 532 (2002) 8.
16. C. Tomei *et al*, GENIUS Collaboration, Proceedings of the IDM 2002 Conference, hep-ph/0306257.
17. The Majorana Collaboration (R. Gaitskell *et al*), White Paper, nucl-ex/0311013.
18. R. Bernabei *et al*, DAMA Collaboration, Riv. N. Cim. 26, n.1 (2003) 1;
    R. Bernabei *et al*, DAMA Collaboration, Phys. Lett. B 480 (2000) 23.
19. B. Ahmed *et al,* UKDM Collaboration, hep-ex/0301039;
    S. Cebrián \etal, Nucl. Phys. Proc. Suppl. 114 (2003) 111.

20. K. Fushimi *et al,* ELEGANT Collaboration, Astrop. Phys. 12 (2000) 185.
21. S.C. Wu *et al*, Nucl. Instr. Meth. A 523 (2004) 116.
22. A. Benoit *et al,* EDELWEISS Collaboration, Phys. Lett. B 545 (2002) 43.
23. D. Abrams *et al*, CDMS Collaboration, Phys. Rev D 66 (2002) 122003.
24. C. Savage, P. Gondolo and K. Freese, astro-ph/0408346;
    A. Kurylov and M. Kamionkowski, astro-ph/0307185;
    P. Ullio, M. Kamionkowski and P. Vogel, JHEP 7 (2001) 44.
25. V.A. Kudryatsev for the UKDM Collaboration, astro-ph/0406126.
26. E. Aprile *et al,* XENON Collaboration, astro-ph/0407575.
27. S. Moriyama for the XMASS Collaboration, IVth Intl. Workshop on the Identification of Dark Matter, York, England, Sept. 2002.
28. R. Brunati *et al*, astro-ph/0405342.
29. K.J. Coakley and D. N. McKinsey, Nucl. Instr. Meth. A 522 (2004) 504.
30. D.S. Akerib *et al,* CDMS Collaboration, astro-ph/0405033, submitted to Phys. Rev. Lett.
31. G. Angloher *et al*, CRESST Collaboration, astro-ph/0408006.
32. G. Angloher *et al,* CRESST Collaboration, Astropart. Phys. 18 (2003) 43.
33. R.W. Schnee, D.S. Akerib and R.J. Gaitskell, astro-ph/0208326.
34. F. Giuliani *et al*, SIMPLE Collaboration, Nucl. Instr. Meth. A526 (2004) 348;
    N. Boukhira *et al,* PICASSO Collaboration, Astropart. Phys. 14 (2000) 227, and hep-ex/0312049.